

vector \mathbf{s}' results from adding a vector $-3\mathbf{b}_1$ to $\mathbf{s}(-3\mathbf{b}_1 + \mathbf{b}_2)$ of equation (8), then

$$\begin{aligned}\mathbf{s}' &= \mathbf{s}(-3\mathbf{b}_1 + \mathbf{b}_2) - 3\mathbf{b}_1 \\ &= (-4 + \frac{1}{3})[\bar{1}10] + \frac{3}{4}[001].\end{aligned}\quad (9)$$

From equation (9) we have calculated that the shift vector of the boundary structure along the boundary plane is $(-4 + \frac{1}{3})[\bar{1}10]$, and that the step height is $\frac{3}{4}[001]$. These two vectors are the same as those obtained from the structure image in Fig. 5.

For the $2H$ structure, the Burgers vector of a GBD was reported to be \mathbf{b}_1 , and the step height to be $[001]_{2H}$ (Takata, Kitano & Komura, 1986). The basis vectors of the DSC-lattice and of the CSL as well as the step vectors of the CSL-pattern are also given in Table 1.

References

ANTERROCHES, C. D' & BOURRET, A. (1984). *Philos. Mag.* **A49**, 783–807.

- BOLLMANN, W. (1970). *Crystal Defects and Crystalline Interfaces*. Berlin: Springer.
- FRIAUF, J. B. (1927a). *Phys. Rev.* **29**, 34–40.
- FRIAUF, J. B. (1927b). *J. Am. Chem. Soc.* **49**, 3107–3114.
- ICHINOSE, H. & ISHIDA, Y. (1981). *Philos. Mag.* **A43**, 1253–1264.
- KING, A. H. & SMITH, D. A. (1980). *Acta Cryst.* **A36**, 335–343.
- KITANO, Y., KOMURA, Y., KAJIWARA, H. & WATANABE, E. (1980). *Acta Cryst.* **A36**, 16–21.
- KITANO, Y., TAKATA, M. & KOMURA, Y. (1986). *J. Microsc.* **142**, 181–189.
- KITANO, Y., TAKATA, M. & KOMURA, Y. (1989). *J. Phys. (Paris)*. In the press.
- KOMURA, Y. (1962). *Acta Cryst.* **15**, 770–778.
- LAVES, F. & WITTE, H. (1935). *Metallwirtsch. Metallwiss. Metalltech.* **14**, 645–649.
- POND, R. C. & BOLLMANN, W. (1979). *Philos. Trans. R. Soc. London Ser. A*, **292**, 449–472.
- POND, R. C. & VLACHAVAS, D. S. (1983). *Proc. R. Soc. London Ser. A*, **386**, 95–143.
- TAKATA, M., KITANO, Y. & KOMURA, Y. (1986). *Trans. Jpn Inst. Met.* **27**(Suppl.), 261–268.
- TAKEDA, S. (1983). *J. Sci. Hiroshima Univ. Ser. A: Math. Phys. Chem.* **46**, 149–194.
- TAKEDA, S., KITANO, Y. & KOMURA, Y. (1983). *J. Electron Microsc.* **32**, 105–114.

Acta Cryst. (1989). **B45**, 13–20

Structure of μ - MnAl_4 with Composition Close to that of Quasicrystal Phases

BY CLARA BRINK SHOEMAKER, DOUGLAS A. KESZLER AND DAVID P. SHOEMAKER

Department of Chemistry, Oregon State University, Corvallis, Oregon 97331, USA

(Received 10 June 1988; accepted 23 August 1988)

Abstract

$\text{MnAl}_{4.12}$, $M_r/100 = 32.43$, $P6_3/mmc$, $a = 19.98$ (1), $c = 24.673$ (4) Å, $V = 8525$ (9) Å³, atoms/cell = 563 (average), $D_x = 3.556$ (2) g cm⁻³, $\lambda(\text{Mo } K\alpha) = 0.71069$ Å, $\mu = 53.05$ cm⁻¹, $F(000) = 8639$, $T = 296$ K, final $R = 0.053$ for 1397 reflections with $I > 2\sigma$. The structure is of interest with relation to quasicrystal phases in the Mn–Al system. Parts of the structure resemble that of φ - $\text{Mn}_3\text{Al}_{10}$. Neither complete Mackay icosahedra (MI), nor 105-atom Bergman clusters are present, but different fragments of MI occur. Most interstices are octahedral, tetrahedral, or trigonal prismatic. The Mn atoms have zero to two Mn atoms in the first coordination shell and four to twelve Mn atoms in the second shell. Of the Mn atoms 108 have icosahedral coordination, two have CN9. Of the 453 Al atoms 6.6% have icosahedral coordination, 35.8% are coordinated by a pentagonal prism of Al atoms with two Mn atoms at the poles, 26.5% have CN13, 25.6% have irregular CN12 arrangements formed by parts of icosahedra and pentagonal prisms, and the remaining 5.5% have other coordinations varying between 11 and

15. Two Al positions are partly occupied. The distance ranges are Mn–Mn 2.678–2.758, Mn–Al 2.359–2.874, Al–Al 2.527–3.166 Å (e.s.d. range: 0.002–0.014 Å). There are almost linear rows of atoms, which center icosahedra or pentagonal prisms. Approximate icosahedral symmetry is propagated in the direction of these rows.

Introduction

A phase of assumed approximate composition MnAl_6 , exhibiting non-crystallographic (icosahedral) symmetry in its electron diffraction pattern, was discovered by Shechtman, Blech, Gratias & Cahn (1984). This phase was formed by extremely rapid cooling from a melt. Subsequently, more non-equilibrium phases have been discovered that exhibit orientational symmetry, but lack periodicity in one or more dimensions; phases of this kind have been called quasicrystalline. Possibly, clues to the structure of a quasicrystalline phase may be provided by the structure of an equilibrium crystalline phase of similar composition. The crystal structure of

MnAl₆ (Nicol, 1953; Kontio & Coppens, 1981) does not seem to provide clues to the structure of the icosahedral phase; none of its atoms is icosahedrally coordinated. Models for the icosahedral Al–Mn phase have been proposed (Elser & Henley, 1985; Guyot & Audier, 1985; Audier & Guyot, 1986) that are based on the Mackay icosahedron (MI) which occurs in the crystal structure of α -(MnAlSi) of composition Mn₂-Al₉Si_{1.8} (Cooper & Robinson, 1966). The MI consists of the first two shells of the icosahedral shell packing described by Mackay (1962). It is a 54-atom unit consisting of an inner icosahedron of Al atoms, surrounded by an outer icosahedron of Mn atoms, with additional Al atoms near the centers of the Mn–Mn edges. Schaefer, Bendersky, Shechtman, Boettinger & Biancianiello (1986) have shown that the quasicrystalline Mn–Al phase may be formed by rapid cooling at a wide composition range, but that single-phase icosahedral material is produced only at compositions close to that of MnAl₄. At higher Mn concentrations and lower cooling rates a decagonal phase is formed. There are two crystalline phases in the Mn–Al system at approximate composition MnAl₄ (Murray, McAlister, Schaefer, Bendersky, Biancianiello & Moffat, 1987), μ and λ , both with large hexagonal unit cells. The crystal structure of the μ phase is the subject of the present paper; that of the λ phase is still under investigation. Henley (1985) has suggested that crystal structures with large unit cells, such as μ and λ , may be rational approximants of a (non-periodic) quasicrystal structure generated by projection from six dimensions. Bendersky (1987) studied the μ phase by electron diffraction, proposed the space group $P6_3/mmc$, and deduced from the similarities between the μ -phase patterns and those of the icosahedral and decagonal phases that the μ phase probably contains icosahedral units, possibly of the MI type, with a twofold axis parallel to the z axis. Dr Bendersky kindly sent us a polycrystalline sample of μ -MnAl₄, from which a single crystal could be isolated for the determination of the structure by X-ray diffraction. A summary report of the results has been published elsewhere (Shoemaker, 1988).

Experimental

A black metallic crystal flake of MnAl₄, approximate dimensions 0.20 × 0.05 × 0.40 mm, was used for the data collection by Molecular Structure Corporation, College Station, TX, with a Rigaku AFC6R diffractometer with graphite-monochromated Mo $K\alpha$ radiation. The ω -scan technique was used, scan rate 16.0° min⁻¹, scan width (0.73 + 0.30 tan θ)°, $2\theta_{\max}$ = 50.1°. The lattice parameters were determined with 25 reflections in the 40.3–48.8° 2θ range. Stationary background counts were recorded on each side of the reflection. The ratio of peak counting time to back-

ground counting time was 2:1. Three standard reflections had an average intensity change of 1.4%. A total of 2975 unique reflections was collected, range h 0–20, k 0–11, l 0–29. Reflections observed: $h, h, l \quad l = 2n$; the highest-symmetry space group was chosen, leading to satisfactory refinement.

Structure determination

The *TEXRAY* system of programs (Molecular Structure Corporation) was used at OSU for the structure determination. There are many high E values, 135 are > 2.0, the largest is 8.1. Straightforward application of direct methods (Gilmore, 1983) did not produce a structure model that would refine to an R factor below 50%. All strong peaks in the Patterson function occur in planes at $z = 0, 0.25, \frac{1}{2}$, and at z values approximately 0.06 and 0.09 from these planes. The strongest peaks on $z = 0, 0.25$ and $\frac{1}{2}$ lie on a triangular grid (the same for the three planes) with sides of the triangles parallel to the x and y axes and with x and y values multiples of about 0.12. This suggests an arrangement of atoms on layers at $z \approx 0.0$ and $\frac{1}{4}$ on a triangular grid, presumably with only part of the nodes occupied. A solution obtained from an E map, followed by successive applications of the program *DIRDIF* (Parthasarathi, Beurskens & Bruins Slot, 1983) showed an icosahedron centered on the mirror plane at $\frac{1}{2}, \frac{1}{2}, \frac{1}{4}$, and an atom on 0, 0, z at 0.31. The atom at 0, 0, 0.31 had apparent coordination 16 (CN16) as occurs in many tetrahedrally close-packed (t.c.p.) alloy structures (Shoemaker & Shoemaker, 1986). This contains a Friauf polyhedron (Samson, 1968) defined by a planar six-ring at $\frac{1}{4}$, a triangle at 0.41 and three other atoms at ≈ 0.32 . This Friauf polyhedron is doubled by the mirror at $\frac{1}{4}$, in the same way as observed in the $C14$ structure type MgZn₂. By successive electron density function refinements this model could be expanded to about the required number of atoms per cell, but the R factor did not drop below 0.54. The model was modified by moving the icosahedron at $\frac{1}{2}, \frac{1}{2}, \frac{1}{4}$ from the mirror plane and centering it on the twofold axis in the $[110]$ direction at $\frac{1}{2}, \frac{1}{2}, \frac{1}{2}$. This gave a Friauf polyhedron around 0, 0, z centred at $z = 0.44$ with a planar six-ring at $z = \frac{1}{2}$. It is now doubled by a symmetry center at 0, 0, $\frac{1}{2}$, in the same way as observed in the $C15$ structure type MgCu₂. These atoms, the atoms forming the icosahedron at $\frac{1}{2}, \frac{1}{2}, \frac{1}{2}$, plus some atoms at $z = 0.34$, generated from this set by vectors having strong peaks in the Patterson function, were used as a starting set for two *DIRDIF* runs. Successive cycles of least squares and electron density maps then led to a plausible structure that could be refined. (After the structure was solved it appeared that one of the original E maps had peaks in the right positions, but with many misleading peak heights which interfered with expansion and refinement).

Refinement

The model was refined by full-matrix least squares. Parameters varied were scale, secondary-extinction coefficient, positional parameters and multiplicities until the Mn/Al assignment was clear. After that, isotropic temperature factors were refined for all atoms, except for Al(11) and Al(17) which appeared to be partly occupied and for which the multiplicities were varied with B fixed at 1.0 \AA^2 . An experimental absorption correction (Walker & Stuart, 1983) was applied which reduced R from 0.12 to 0.10; correction factors on I : 0.84–1.32. Final $R = 0.053$, $wR = 0.072$, $S = 1.47$, 1397 reflections with $I > 2\sigma$, 127 variables. (For all 2824 reflections, $R = 0.139$, $wR = 0.079$, $S = 1.40$). Quantity minimized was $\sum w(F_o - F_c)^2$ with $w^{-1} = \sigma^2(F)$, based on $\sigma^2(F^2)$ as determined by counting statistics plus a contribution of $(0.05F^2)^2$. $(\Delta/\sigma)_{\max} = 0.211$ for $x[\text{Al}(32)]$, which was still oscillating, $(\Delta/\sigma)_{\text{mean}} = 0.003$. Final $\Delta\rho$ excursions -1.5 to $+2.1 \text{ e \AA}^{-3}$ [near the partially occupied Al(11) site]. The scattering factors and anomalous-dispersion corrections were taken from *International Tables for X-ray Crystallography* (1974). The final parameters are listed in Table 1.* The largest (isotropic) secondary-extinction correction was 35%.

There are ten Mn sites and 32 Al sites. The occupancy factor for atom Al(11) indicates that there are 5.09 (12) atoms on a site of multiplicity 12. Figs. 1(a) and 2(a) show that the two positions for Al(11) cannot be simultaneously occupied. The Al(17) site of multiplicity 12 is occupied by 8.06 (14) atoms; complete occupancy would result in somewhat short but acceptable distances. The total number of Al atoms is thus 453 (which could be increased to 458 with highest possible occupancies), and the total number of Mn atoms is 110, leading to the formula $\text{MnAl}_{4.12}$.

Description of the structure

The structure is shown in Fig. 1 in layers perpendicular to the z axis. The layer at $z = \frac{1}{4}$ is located in a mirror plane and therefore planar; the one centered at $z = \frac{1}{2}$ is almost planar, although not required to be so by symmetry. The layers centered at 0.325 and 0.425 are considerably puckered. The layers centered at $z = 0.575$, 0.675 and $\frac{3}{4}$ (not shown) are generated from the layers centered at $z = 0.425$, 0.325 and $\frac{1}{4}$, respectively, by the operation of the twofold axis at $z = \frac{1}{2}$ in the $[110]$ direction. Since the layer at 0.425 has a pseudo-twofold axis in that direction, the layer at $\frac{1}{2}$ is a pseudo-mirror with respect to its adjacent layers.

* Lists of structure factors and interatomic distances have been deposited with the British Library Document Supply Centre as Supplementary Publication No. SUP 51285 (14 pp.). Copies may be obtained through The Executive Secretary, International Union of Crystallography, 5 Abbey Square, Chester CH1 2HU, England.

Table 1. Positional parameters, B_{eq} values and occupancy factors for $\mu\text{-MnAl}_{4.12}$

	Site	x	y	z	$B_{\text{eq}} (\text{\AA}^2)$	Occ.
Mn(1)	2(b)	0	0	$\frac{1}{4}$	0.74 (13)	
Mn(2)	12(f)	0.24315 (16)	0.00231 (18)	$\frac{1}{4}$	0.99 (5)	
Mn(3)	12(f)	0.37826 (15)	-0.00123 (17)	$\frac{1}{4}$	0.81 (5)	
Mn(4)	6(h)	-0.62081 (23)	0.62081	$\frac{1}{4}$	0.87 (7)	
Mn(5)	6(h)	0.50630 (23)	0.25315	$\frac{1}{4}$	0.80 (7)	
Mn(6)	12(k)	0.41538 (15)	0.20769	0.33787 (9)	0.75 (4)	
Mn(7)	12(k)	0.07909 (17)	-0.07909	0.41225 (9)	0.78 (5)	
Mn(8)	12(k)	0.45976 (17)	-0.45976	0.41286 (9)	0.80 (5)	
Mn(9)	12(k)	0.25404 (16)	0.12702	0.49840 (9)	0.77 (5)	
Mn(10)	24(l)	0.49545 (10)	0.36903 (10)	0.49795 (7)	0.67 (4)	
Al(11)	12(f)	0.13345 (71)	0.04238 (66)	$\frac{1}{4}$	1.0	0.424 (10)
Al(12)	6(h)	0.12167 (50)	-0.12167	$\frac{1}{4}$	1.29 (14)	
Al(13)	12(f)	0.12891 (33)	0.49139 (32)	$\frac{1}{4}$	1.09 (10)	
Al(14)	6(h)	0.51015 (42)	-0.51015	$\frac{1}{4}$	0.83 (13)	
Al(15)	12(f)	0.37677 (32)	0.12434 (28)	$\frac{1}{4}$	0.80 (9)	
Al(16)	6(h)	0.61909 (45)	-0.61909	$\frac{1}{4}$	0.77 (14)	
Al(17)	12(k)	0.04315 (44)	-0.04315	0.32664 (29)	1.0	0.672 (12)
Al(18)	24(l)	0.18052 (21)	0.20495 (22)	0.34061 (15)	1.29 (7)	
Al(19)	12(k)	0.26302 (31)	0.13151	0.30657 (19)	0.87 (9)	
Al(20)	24(l)	0.33588 (20)	0.05052 (19)	0.34360 (14)	0.87 (6)	
Al(21)	24(l)	0.10759 (21)	0.36195 (22)	0.30753 (13)	1.07 (6)	
Al(22)	12(k)	0.25491 (34)	-0.25491	0.30781 (21)	1.15 (10)	
Al(23)	12(k)	0.57088 (30)	0.28544	0.34688 (21)	1.07 (9)	
Al(24)	24(l)	0.49104 (21)	0.13061 (22)	0.30761 (13)	0.95 (7)	
Al(25)	24(l)	0.02882 (20)	0.44214 (20)	0.34077 (14)	0.98 (6)	
Al(26)	12(k)	-0.58834 (31)	0.58834	0.34024 (19)	0.82 (9)	
Al(27)	4(f)	$\frac{1}{4}$	$-\frac{1}{4}$	0.33971 (36)	0.89 (16)	
Al(28)	4(e)	0	0	0.43376 (36)	1.12 (17)	
Al(29)	24(l)	0.23620 (22)	-0.00056 (25)	0.44251 (13)	0.93 (6)	
Al(30)	12(k)	0.15636 (35)	0.07818	0.40420 (20)	1.05 (9)	
Al(31)	12(k)	0.31601 (30)	0.15800	0.40936 (19)	0.92 (10)	
Al(32)	12(k)	0.15687 (30)	-0.15687	0.40280 (21)	1.09 (10)	
Al(33)	24(l)	0.15748 (22)	0.46151 (22)	0.40260 (14)	1.03 (7)	
Al(34)	12(k)	-0.61573 (33)	0.61573	0.44306 (20)	1.05 (10)	
Al(35)	24(l)	0.38466 (20)	-0.00201 (23)	0.44333 (14)	0.82 (6)	
Al(36)	24(l)	0.45985 (22)	0.15706 (22)	0.41052 (13)	0.86 (7)	
Al(37)	12(k)	0.61805 (33)	-0.61805	0.44247 (20)	1.02 (10)	
Al(38)	12(k)	0.53926 (35)	-0.53926	0.40681 (18)	0.86 (9)	
Al(39)	12(i)	0.12651 (24)	0	$\frac{1}{4}$	0.94 (10)	
Al(40)	24(l)	0.10969 (22)	0.36518 (22)	0.49580 (14)	1.04 (7)	
Al(41)	12(k)	0.25446 (32)	-0.25446	0.49544 (20)	0.90 (10)	
Al(42)	6(g)	$\frac{1}{4}$	0	$\frac{1}{4}$	1.00 (14)	

The layers centered at $\frac{1}{4}$ and $\frac{1}{2}$ are very similar and show the triangular arrangement expected from the Patterson function, but with large apparent holes. The holes are of two kinds. The threefold symmetry of the larger holes is perfect on the layer centered at $z = \frac{1}{2}$, but approximate on $z = \frac{1}{4}$. The smaller holes have a twofold axis in the direction of their long axes on $z \approx \frac{1}{2}$, and a mirror perpendicular to their long axes on $z = \frac{1}{4}$. Both apparent holes are partially filled in by atoms (at a distance of about 0.06c from the plane of the hole) in the puckered layers above and below. On both layers three atoms from above and below a threefold hole form a trigonal prism, and two atoms from above and below the smaller hole form an octahedron with two atoms surrounding the hole (e.g. atoms 14 and 16 on $z = \frac{1}{4}$).

There is a strong resemblance of parts of the structure with the structure of $\varphi\text{-Mn}_3\text{Al}_{10}$ (Taylor, 1959), which has the same space group, $a = 7.543$ (1), $c = 7.898$ (1) \AA . The outline of the repeat unit for the layers at $z \approx 0$, $\frac{1}{2}$ in the φ phase (Pearson, 1972) is indicated by dashed lines on the μ layer at $z \approx 0.425$, and for the φ layer at $z = \frac{1}{4}$ on the μ layer centered at $\frac{1}{2}$. The resemblance continues on the next layer above. The apparent holes in the φ layer in the mirror plane are all

of the threefold type and three atoms above and below the plane form a trigonal prism, which in this case is also empty. The Co₂Al₅ structure (Newkirk, Black & Damjanovic, 1961) differs from the φ phase in that the trigonal prism is filled with a transition-metal atom.

In the φ phase the atoms surrounding the atom at a cell corner [corresponding with atom Mn(08) on the μ layer at 0.425] lie on almost perfect concentric circles (disregarding the small differences in z), but in the μ phase these circles are elongated in the [110] direction and centered between atoms Mn(08) and Al(38). (The inner circle is formed by atoms 37, 36, 35, 33, 34, 33, 35, 36.) A similar chunk of modified φ phase may be recognized on the μ layer at $\frac{1}{4}$ and adjacent layers. The resemblance here is even stronger: there are *elliptical*

rings of atoms on $z \simeq 0.325$, centered between atoms Mn(06) and Al(20) (less regular where the ring comes close to the origin of the unit cell) but there are also *circular* rings of atoms, as in the φ phase, surrounding Al(27) (again neglecting the small difference in z of the atoms).

A recurrent feature on the layers at $z = \frac{1}{4}$ and $\simeq \frac{1}{2}$ is a group of six atoms, three Mn atoms forming a large triangle and three Al atoms with centers slightly outside the sides of this triangle. In all these cases there are three Al atoms, above and below, forming two octahedra with the three Al atoms in the plane. In three cases another Mn atom in the following layer completes a large tetrahedron with as base the three Mn atoms in the layers at $z = \frac{1}{4}$ or $z \simeq \frac{1}{2}$. These tetrahedra

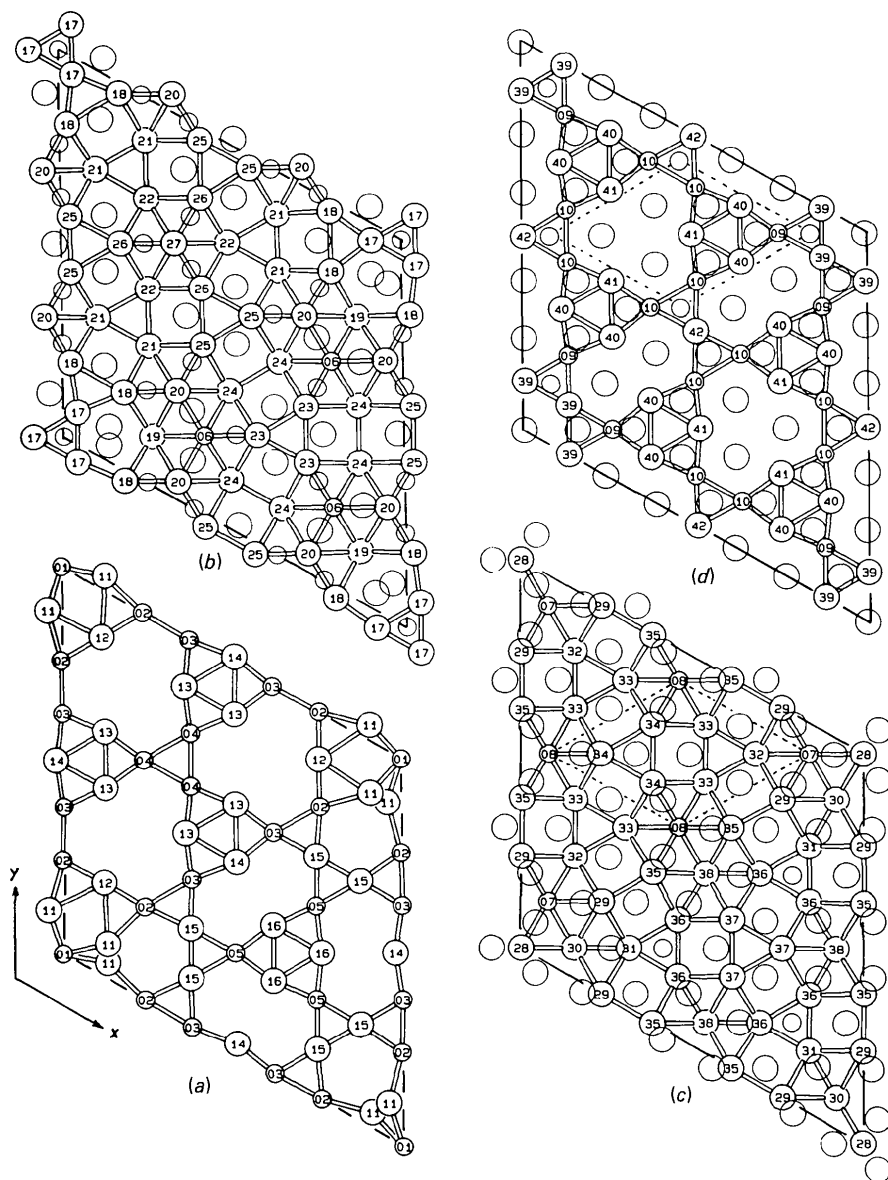


Fig. 1. Layers in the μ -MnAl_{4.12} crystal structure perpendicular to the z axis (adapted from Fig. 1 of Shoemaker, 1988). Other layers are generated by the operation of the mirror plane at $z = \frac{1}{4}$ perpendicular to the z axis, and the twofold axis at $z = \frac{1}{2}$ in the [110] direction. Layers centered at 0.325 and 0.425 are considerably puckered. Small circles, numbered from 01 to 10, represent Mn atoms; large circles, numbered from 11 to 42, represent Al atoms. (a) Layer in the mirror plane at $z = \frac{1}{4}$. (b) Puckered layer at $z = 0.325 \pm 0.025$. Atoms at $\frac{1}{4}$ are shown unconnected and unnumbered; their numbers can be found on (a). (c) Puckered layer at $z = 0.425 \pm 0.025$. Atoms at $\simeq 0.325$ are shown unconnected and unnumbered; their numbers can be found on (b). (d) Almost planar layer at $z = 0.500 \pm 0.005$. Atoms at $\simeq 0.425$ are shown unconnected and unnumbered; their numbers can be found on (c).

have Al atoms of one of the octahedra mentioned above slightly outside all six edges. They are formed by Mn atoms 3, 3, 4, 8 and Mn atoms 1, 2, 2, 7 (base on $z = \frac{1}{4}$, top on 0.425), and by Mn atoms 10, 10, 9, 6 (base on $z \approx \frac{1}{2}$, top on 0.325 or 0.675). The arrangement of the atoms near the origin is distorted, in particular the octahedron formed by atoms 17, 18, 18 and 11, 11, 12 inside the tetrahedron 1, 2, 2, 7 (see below). The tetrahedra with their base on $\frac{1}{4}$ are doubled by the operation of the mirror plane. The triangle formed by atoms Mn(5) on $z = \frac{1}{4}$ has no Mn top on $z \sim 0.425$, but instead a triangle formed by atoms Al(37).

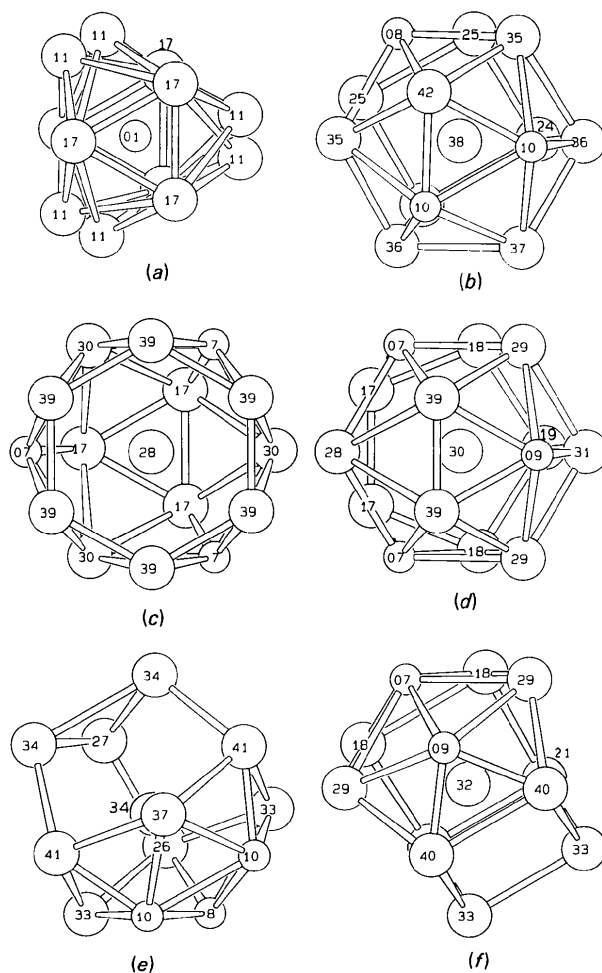


Fig. 2. Some coordination polyhedra for μ -MnAl_{4.12}. (a) Trigonal prism of Al, with half occupied Al(11) sites outside the quadrangular faces, for Mn(1). (b) CN13 coordination for Al(38). Other atoms in Table 4 have similar coordination. (c) Friauf polyhedron plus three Al(30) atoms outside planar six-membered rings for Al(28). Another Al(28), outside the Al(39) six-membered ring, is at a larger distance and is not shown. (d) CN14 (distorted t.c.p. CN16) polyhedron for Al(30). (e) Irregular CN12 polyhedron for Al(34). (f) Irregular CN12 polyhedron for Al(32). Other atoms in Table 5 have similar coordination.

Table 2. Number of near neighbors (N) and distances in Å (< 3.2 Å) for atoms with icosahedral coordination

The ranges of estimated standard deviations (in Å) in the distances listed in this table and following tables are: Mn–Mn 0.003–0.007, Mn–Al 0.002–0.008, Al–Al 0.004–0.014 [for distances involving Al(11) the standard deviations are 0.012].

	N	Mn	N	Al
Mn(2)	1	2.735	11	2.452–2.812
Mn(3)	1	2.735	11	2.408–2.846
Mn(4)	2	2.748	10	2.436–2.759
Mn(5)	2	2.678	10	2.417–2.713
Mn(6)	1	2.678	11	2.434–2.747
Mn(7)	1	2.758	11	2.451–2.819
Mn(8)	2	2.703	10	2.445–2.761
Mn(9)	1	2.758	11	2.416–2.874
Mn(10)	2	2.703, 2.707	10	2.440–2.760
Al(15)	5	2.523–2.605	7	2.559–2.731
Al(39)	4	2.543–2.566	8	2.527–3.010
Al(42)	6	2.562–2.573	6	2.671–2.678

Atomic coordinations

Although there are 42 kinds of atoms per cell, only a limited number of coordination types occur.

Mn coordinations. The Mn atoms occurring at the corners of the triangular and tetrahedral clusters described above are coordinated by icosahedra (see Table 2). The atoms at the base of the tetrahedra have a *twofold* axis parallel to z , the atom at the apex a *threefold* axis. Mn(1) does not have icosahedral coordination, it is surrounded by a trigonal prism of Al with three of the six disordered Al(11) atoms outside the rectangular faces (see Fig. 2a). Table 6 shows that all vertices of the Mn(1) polyhedron are partially occupied. The distances for Mn(1) are the shortest [2.359 (12) Å] and insignificantly different from the next-shortest [2.409 (7) Å] Mn–Al distances in the structure. Short Mn–Al distances have been reported before: in the α -(AlMnSi) phase (Cooper & Robinson, 1966) the shortest Mn–Al distance is 2.27 (3) Å. In the recently redetermined structure of MnAl₆ (Kontio & Coppens, 1981) the shortest Mn–Al distance is 2.455 (1) Å.

The Mn atoms have from zero to two Mn atoms (average 1.4) in their first coordination shell and from four to twelve Mn atoms (average 7.0) in their second coordination shell at distances from 4.336 to 5.145 Å.

Al coordinations. The coordinations of the Al atoms depend on the number and the location of the Mn atoms in their first coordination shell. Three Al atoms with between four and six Mn near-neighbors have icosahedral coordination and are listed in Table 2. They are on the long axes of the small holes on layers $\frac{1}{4}$ [Al(15)] and $\frac{1}{2}$ [Al(39) and Al(42)]. (This last atom and its surrounding icosahedron were used in the derivation of the structure.) The other Al atoms have between two and three Mn neighbors and their coordination polyhedra are either bicapped pentagonal prisms, or a combination of icosahedra and pentagonal prisms.

All Al atoms forming part of the tetrahedral clusters are surrounded by ten Al atoms at the corners of a

pentagonal prism with two Mn atoms of the tetrahedron on the prism axis. The direction of the fivefold axes of the prisms is thus along the edges of the tetrahedra. For the atoms in the layers $\frac{1}{4}$ and $\approx\frac{1}{2}$ this direction is perpendicular to z ; for the atoms on the puckered layers this axis makes an angle of about 35° with z (Table 3). For example, for atom Al(25) the five-membered rings of the pentagonal prism are formed respectively by atoms 26, 25, 38, 35, 33 and 13, 14, 24, 20, 21. The surroundings are different for the atoms near the origin; atom Al(11) (occupancy about $\frac{1}{2}$ has an irregular CN11, and atom Al(17) (occupancy about $\frac{2}{3}$) is surrounded by an icosahedron missing one vertex (see Table 6).

Al atoms with CN13 are listed in Table 4. The atoms with Schläfli symbols 3^6 (on the axes of the elliptical rings of atoms described above) and 4^23^3 (the pairs of atoms filling in the smaller holes on layers $\frac{1}{4}$ and $\frac{1}{2}$) have three Mn near neighbors, two of which are adjacent. Their polyhedron has 13 triangular, three quadrangular and one pentagonal face, see Fig. 2(b). Atom Al(19) with Schläfli symbol 3^45 has three non-adjacent Mn neighbors and a somewhat different CN13 polyhedron with one vertex partially occupied.

Table 5 lists Al atoms that have an irregular CN12, formed by part of an icosahedron and part of a pentagonal prism. These atoms have two adjacent Mn atoms in their first coordination shell, which accounts for the icosahedral part of their CN. The polyhedron has three quadrangular faces, two non-planar pentagonal faces and eight triangular faces, as shown in Fig. 2(f). The Schläfli symbol for these atoms is 3^2434 . Other atoms with this same symbol are the Al atoms of the tetrahedral clusters on the puckered layers and have already been listed in Table 3. Atom Al(34) has three Mn neighbors and has a different irregular CN12 shown in Fig. 2(e).

Some miscellaneous coordinations are listed in Table 6. The CN's for atoms Mn(1), Al(11), Al(17) and Al(34) have already been mentioned above. Al(27), with symmetry $3m$, is coordinated by a trigonal prism with six atoms around the centre as in hexagonal close packing. Atom Al(28), shown in Fig. 2(c), is surrounded by the t.c.p. CN16 polyhedron used in the derivation of the structure, although the atom Al(28) outside the six-membered ring at $z = \frac{1}{2}$ is somewhat farther away (3.267 Å) and not shown in the figure. Atom Al(30), shown in Fig. 2(d), is connected to Al(28) by a six-coordinated bond. It has CN14, formed from a t.c.p. CN16 by replacing one six-membered face of the Friauf polyhedron and the atom outside that face by a five-membered ring (atoms 18, 17, 17, 18, 19).

The shortest Al–Al distance in the structure is 2.527 (5) Å. The shortest Al–Al distance in the α -(AlMnSi) phase (Cooper & Robinson, 1966) is 2.44 (4) Å and in MnAl₆ (Kontio & Coppens, 1981) 2.539 (1) Å.

Table 3. *Near neighbors and distances in Å (< 3.2 Å) for Al atoms coordinated by a pentagonal prism of Al atoms with two Mn atoms at the poles*

Asterisks mark cases where the approximate fivefold axis of the pentagonal prism is perpendicular to the z axis.

	2 Mn	10 Al
Al(12)*	2 Mn(2): 2.452	2.805–3.166
Al(13)*	Mn(3): 2.408, Mn(4): 2.436	2.753–2.965
Al(14)*	2 Mn(3): 2.448	2.797–2.965
Al(16)*	2 Mn(5): 2.417	2.772–2.905
Al(18)	Mn(2): 2.486, Mn(7): 2.492	2.600–3.118
Al(25)	Mn(8): 2.459, Mn(3): 2.489	2.706–2.937
Al(26)	Mn(8): 2.445, Mn(4): 2.494	2.708–2.937
Al(31)	Mn(9): 2.445, Mn(6): 2.463	2.697–2.884
Al(36)	Mn(6): 2.434, Mn(10): 2.443	2.728–2.911
Al(40)*	Mn(9): 2.416, Mn(10): 2.457	2.722–2.913
Al(41)*	2 Mn(10): 2.440	2.723–2.882

Table 4. *Near neighbors and distances in Å (< 3.2 Å) for Al atoms with CN13*

Of the three Mn neighbors two are adjacent, except for Al(19) (see Fig. 2b).

	Schläfli symbol	3 Mn	10 Al
Al(19)	3^45	2.747, 2.783 (2×)	2.685–3.034
Al(20)	3^6	2.723, 2.812, 2.827	2.640–3.021
Al(24)	4^23^3	2.713, 2.746, 2.846	2.638–3.001
Al(29)	4^23^3	2.760, 2.785, 2.819	2.615–2.988
Al(35)	4^23^3	2.756, 2.760, 2.761	2.678–3.021
Al(38)	3^6	2.752 (2×), 2.755	2.671–3.001

Table 5. *Near neighbors and distances in Å (< 3.2 Å) for Al atoms with irregular CN12*

The two Mn neighbors are adjacent. Schläfli symbol for all atoms is 3^2434 (see Fig. 2f).

	2 Mn	10 Al
Al(21)	2.716, 2.720	2.789–2.948
Al(22)	2.759 (2×)	2.753–2.948
Al(23)	2.638, 2.699	2.849–2.905
Al(32)	2.647, 2.701	2.860–2.946
Al(33)	2.699, 2.706	2.822–2.946
Al(37)	2.703 (2×)	2.825–2.914

Discussion

Contrary to expectations (Bendersky, 1987) no complete MI is present in the structure, although there are many areas where the atoms are arranged as in parts of an MI with its center occupied by a Mn atom. The large Mn triangles on layers $\frac{1}{4}$ and $\approx\frac{1}{2}$ with the associated Al octahedra above and below occur in this MI. The Al atoms inside such an MI are coordinated by pentagonal prisms of Al atoms with two Mn atoms at the poles. In fact, the double tetrahedron with common base 3, 3, 4 and its associated Al atoms accounts for a large part of the atoms in an MI [positioned with a twofold axis parallel to z , as Bendersky (1987) suggested for the icosahedral units], plus atoms beyond its boundary generated by a vertical (pseudo-) threefold axis of the double tetrahedron. Some Al atoms of the MI are replaced by Mn atoms in the μ phase, where Mn–Mn nearest neighbors, which are absent in α -(MnAlSi) (Cooper & Robinson, 1966), do occur.

Table 6. *Coordination numbers, near-neighbor distances in Å (< 3.2 Å) and coordination polyhedra for atoms with miscellaneous coordinations (see Figs. 2a,c-e)*

	CN	Mn	Al	Polyhedron
Mn(1)	9	—	9 Al: 2.359–2.409	Trigonal prism + 3, all vertices partially occupied
Al(11)	11	Mn(1): 2.359 Mn(2): 2.683	9 Al: 2.582–3.166	$\approx \frac{1}{2}$ occupied, irregular, 4 vertices $\frac{1}{3}$ occupied
Al(17)	11	Mn(1): 2.409 Mn(7): 2.451	9 Al: 2.582–3.036	$\approx \frac{2}{3}$ occupied, icosahedron minus one vertex, 6 vertices partially occupied
Al(27)	12	3 Mn(4): 2.723	9 Al: 2.709–3.100	Trigonal prism + 6 (h.c.p.)
Al(28)	15	3 Mn(7): 2.788	12 Al: 2.802–3.036	T.c.p. CN16, one vertex, Al(28), at 3.267 Å, 3 vertices partially occupied
Al(30)	14	2 Mn(7): 2.728 1 Mn(9): 2.874	11 Al: 2.729–3.034	Distorted t.c.p. CN16, 2 vertices partially occupied
Al(34)	12	2 Mn(10): 2.693 1 Mn(8): 2.716	9 Al: 2.708–3.100	Irregular CN12, 10 triangular, 3 pentagonal faces

The 105-atom cluster occurring in the crystal structure of $Mg_{32}(Si,Al)_{49}$ and the isostructural Al_3CuLi_3 (Bergman, Waugh & Pauling, 1957), which we will call the Bergman cluster (BC), has been used in models of the quasicrystal phases formed at approximately the composition of the crystal phases by Henley & Elser (1986) and Audier, Sainfort & Dubost (1986), as well as in an alternative icosatwin model by Pauling (1987). In the BC all interstices are tetrahedral and the central icosahedron is interpenetrated by twelve icosahedra. In μ - $MnAl_4$ the largest concentration of tetrahedral interstices is in the surroundings of the Al atoms with icosahedral coordination. But even these icosahedra are interpenetrated by at most six other icosahedra, and therefore a BC does not occur in the μ phase.

There is an intriguing similarity between the arrangement of some of the atoms in the μ phase and the high-resolution electron-microscope (HREM) images along a twelvefold axis of a dodecagonal phase, recently observed by Chen, Li & Kuo (1988). This phase is formed by rapid solidification of V_3Ni_2 and $V_{15}Ni_{10}Si$, is periodic along the twelvefold axis and has about the same composition as the t.c.p. σ phase (Bergman & Shoemaker, 1954). The HREM images show circular rings of spots surrounding a central hexagon, as observed for the atoms in the ϕ phase on $z \approx 0$ and on the 0.325 layer of the μ phase, and also elliptical rings of spots surrounding a double hexagon, as found for the arrangement of atoms in both puckered layers of the μ phase. However, the similarity is fortuitous: in both cases the patterns observed are tessellations of triangles and quadrangles, but in the HREM images they are not formed by near neighbors, but by second-nearest neighbors, corresponding with the less-dense secondary nets of a t.c.p. structure.

Other quasicrystal phases have been discovered in systems at compositions close to stable t.c.p. phases (Kuo, 1986; Kuo, Zhou & Li, 1987). We have

proposed that the propagation of icosahedral symmetry that must be essential for the formation of an icosahedral phase, may be related to the occurrence of rows of interpenetrating icosahedra in the t.c.p. phases (Shoemaker & Shoemaker, 1987). In the μ phase on layers centered at $z = \frac{1}{4}$ and $\frac{1}{2}$ there occur almost linear rows of atoms in the directions of the cell edges (and [110]). These atoms center icosahedra (twofold axes parallel to z) or pentagonal prisms, which interpenetrate by sharing five-membered rings of atoms. The pentagonal prisms introduce octahedral interstices in the structure, common to structures containing a large number of Al atoms. Most of the atoms of these rows are part of the triangular clusters mentioned above. Although these rows are not quite linear, approximate icosahedral symmetry is propagated in their average direction.

We wish to thank Dr C. L. Henley for suggesting the problem and Dr L. A. Bendersky for providing the sample. The X-ray facility at Oregon State University was established with funds provided by the US National Science Foundation (CHE-8604239) and by the Four-sight! program of the OSU Foundation.

References

- AUDIER, M. & GUYOT, P. (1986). *Philos. Mag. B*, **53**, L43–L51.
 AUDIER, M., SAINFORT, P. & DUBOST, B. (1986). *Philos. Mag. B*, **54**, L105–L111.
 BENDERSKY, L. (1987). *J. Microsc.* **146**, 303–312.
 BERGMAN, G. & SHOEMAKER, D. P. (1954). *Acta Cryst.* **7**, 857–865.
 BERGMAN, G., WAUGH, J. L. T. & PAULING, L. (1957). *Acta Cryst.* **10**, 254–259.
 CHEN, H., LI, D. X. & KUO, K. H. (1988). *Phys. Rev. Lett.* **60**, 1645–1648.
 COOPER, M. & ROBINSON, K. (1966). *Acta Cryst.* **20**, 614–617.
 ELSER, V. & HENLEY, C. L. (1985). *Phys. Rev. Lett.* **55**, 2883–2886.
 GILMORE, G. T. (1983). *MITHRIL. A Computer Program for the Automatic Solution of Crystal Structures from X-ray Data*. Univ. of Glasgow, Scotland.
 GUYOT, P. & AUDIER, M. (1985). *Philos. Mag. B*, **52**, L15–L19.
 HENLEY, C. L. (1985). *J. Non-Cryst. Solids*, **75**, 91–96.
 HENLEY, C. L. & ELSER, V. (1986). *Philos. Mag. B*, **53**, L59–L66.
International Tables for X-ray Crystallography (1974). Vol. IV, pp. 71, 148. Birmingham: Kynoch Press. (Present distributor Kluwer Academic Publishers, Dordrecht.)
 KONTIO, A. & COPPENS, P. (1981). *Acta Cryst.* **B37**, 433–435.
 KUO, K. H. (1986). *J. Phys. (Paris)*, **47**, C3-425–436.
 KUO, K. H., ZHOU, D. S. & LI, D. X. (1987). *Philos. Mag. Lett.* **55**, 33–39.
 MACKAY, A. L. (1962). *Acta Cryst.* **15**, 916–918.
 MURRAY, J. L., MCALISTER, A. J., SCHAEFER, R. J., BENDERSKY, L. A., BIANCANIELLO, F. S. & MOFFAT, D. L. (1987). *Metall. Trans. A*, **18**, 385–392.
 NEWKIRK, J. B., BLACK, P. J. & DAMJANOVIC, A. (1961). *Acta Cryst.* **14**, 532–533.
 NICOL, A. D. I. (1953). *Acta Cryst.* **6**, 285–292.
 PARTHASARATHI, V., BEURSKENS, P. T. & BRUINS SLOT, H. J. (1983). *Acta Cryst.* **A39**, 860–864.

- PAULING, L. (1987). *Phys. Rev. Lett.* **58**, 365–368.
- PEARSON, W. B. (1972). *The Crystal Chemistry and Physics of Metals and Alloys*, p. 552. New York: Wiley-Interscience.
- SAMSON, S. (1968). *Structural Chemistry and Molecular Biology*, edited by A. RICH & N. DAVIDSON, pp. 687–717. San Francisco: Freeman.
- SCHAEFER, R. J., BENDERSKY, L. A., SHECHTMAN, D., BOETTINGER, W. J. & BIANCANIELLO, F. S. (1986). *Metall. Trans. A*, **17**, 2117–2125.
- SHECHTMAN, D., BLECH, I., GRATIAS, D. & CAHN, J. W. (1984). *Phys. Rev. Lett.* **53**, 1951–1954.
- SHOEMAKER, C. B. (1988). *Phys. Rev. B*. In the press.
- SHOEMAKER, D. P. & SHOEMAKER, C. B. (1986). *Acta Cryst.* **B42**, 3–11.
- SHOEMAKER, D. P. & SHOEMAKER, C. B. (1987). *Mater. Sci. Forum*, **22–24**, 67–82.
- TAYLOR, M. A. (1959). *Acta Cryst.* **12**, 393–396.
- WALKER, N. & STUART, D. (1983). *Acta Cryst.* **A39**, 158–166.

Acta Cryst. (1989). **B45**, 20–26

Study of the Incommensurately Modulated Structure of Cs₂CdBr₄ by Single-Crystal Diffraction

BY NIVALDO L. SPEZIALI† AND GERVAIS CHAPUIS

Université de Lausanne, Institut de Cristallographie, BSP, Dorigny, 1015 Lausanne, Switzerland

(Received 22 April 1988; accepted 22 July 1988)

Abstract

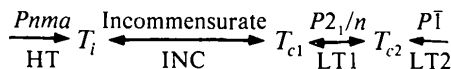
Three thermotropic phase transitions have been detected in Cs₂CdBr₄: a second-order orthorhombic to incommensurate transition at $T_i = 252$ K, a first-order incommensurate to monoclinic transition at $T_{c1} = 237$ K and a second-order monoclinic to triclinic transition at $T_{c2} = 156$ K. The incommensurate phase of Cs₂CdBr₄ has been studied by single-crystal X-ray diffraction. Main reflections and first-order satellites were measured at 245 K. Based on extinction rules for the diffracted intensities, the superspace group could be determined unambiguously. The modulation vector could be precisely measured as $\mathbf{q} = 0.170(3)\mathbf{a}^*$. The incommensurately modulated structure is characterized by a rotation of the CdBr₄ tetrahedra around \mathbf{a} in addition to a slight translational component along \mathbf{b} . In the monoclinic phase the rotation of the tetrahedra is 'locked' and the structure analysis shows the existence of two twinning domains. Crystal data: dicaesium tetrabromocadmate, Cs₂CdBr₄, $M_r = 697.9$. At 245 K: $Pnma$, $a = 10.205(4)$, $b = 7.887(3)$, $c = 13.925(7)$ Å, $\lambda(\text{Cu } K\alpha) = 1.5418$ Å, $R = 0.054$ for 578 reflections. At 200 K: $P2_1/n$, $a = 10.200(3)$, $b = 7.844(4)$, $c = 13.958(9)$ Å, $\alpha = 90.0(1)^\circ$, $\lambda(\text{Mo } K\alpha) = 0.71069$ Å, $R = 0.042$ for 1739 reflections.

1. Introduction

The room-temperature phase of Cs₂CdBr₄ is isomorphous with β -K₂SO₄ (orthorhombic space group $Pnma$) with $a = 10.228(7)$, $b = 7.931(4)$ and $c = 13.966(8)$ Å and four formula units per unit cell

† Permanent address: Departamento de Física, Universidade Federal de Minas Gerais, 30161 Belo Horizonte, Brazil.

(Altermatt, Arend, Gramlich, Niggli & Petter, 1984). With decreasing temperature the crystal undergoes a displacive-type structural phase transition at $T_i = 252$ K into an incommensurate phase as evidenced by the presence of satellite reflections on diffractograms. Two additional phase transitions take place at $T_{c1} = 237$ K, a first-order phase transition, and at $T_{c2} = 156$ K, a second-order phase transition:



Studies based on ⁸¹Br nuclear quadrupolar resonance measurements (Plesko, Kind & Arend, 1980) revealed the existence of the above phase-transition sequence. Their results were also in agreement with the symmetry detected by X-ray diffraction for the normal and commensurate phases. No ferroelectric phase occurs for Cs₂CdBr₄ as it does in other A_2BX_4 -type compounds like K₂SeO₄ (Izumi, Axe & Shirane, 1977) and Rb₂ZnCl₄ and Rb₂ZnBr₄ halides (Sawada, Shiroishi, Yamamoto, Takashige & Matsuo, 1978; Arend, Muralt, Plesko & Altermatt, 1980) for example. Studies by Maeda, Honda & Yamada (1983) showed that by lowering the temperature, the intensity of the satellite reflection 0311 behaves like $I \propto (T_i - T)^\beta$ with $\beta = 0.29$. In addition, they detected a linear decrease of the q value from 0.15 to 0.20 with decreasing temperature. The superspace group of the INC phase discussed by other authors seemed to be controversial (Maeda *et al.*, 1983; Altermatt *et al.*, 1984).

No structural study of the incommensurate phase of this compound has been performed. The small value of q causes the satellites to be very close to the main reflections. This fact together with the low intensities of the satellite reflections and the high absorption